Geophysical Research Letters

RESEARCH LETTER

10.1029/2020GL088924

Atmospheric Gravity Waves Observed in the Nightglow Following the 21 August 2017 Total Solar Eclipse

I. Paulino[1], C. A. O. B. Figueiredo[2], F. S. Rodrigues[3], R. A. Buriti[1], C. M. Wrasse[2], A. R. Paulino[4], D. Barros[2], H. Takahashi[2], I. S. Batista[2], A. F. Medeiros[1], P. P. Batista[2], M. A. Abdu[2], E. R. de Paula[2], C. M. Denardini[2], L. M. Lima[4], R. Y.C. Cueva[5], and J. J. Makela[6]

[1]Unidade Acadêmica de Física, Universidade Federal de Campina Grande, Campina Grande, Brazil, [2]Instituto Nacional de Pesquisas Espaciais, São José dos Campos, Brazil, [3]W. B. Hanson Center for Space Sciences, University of Texas at Dallas, Richardson, TX, USA, [4]Departamento de Física, Universidade Estadual da Paraíba, Campina Grande, Brazil, [5]Departamento de Física, Universidade Estadual do Maranhão, São Luís, Brazil, [6]Department of Electrical and Computing Engineering, University of Illinois, Urbana-Champaign, IL, USA

Key Points:
- A multi-instrumented observational campaign was carried out in Brazil to study the effects of the 21 August 2017 solar eclipse
- Atmospheric gravity waves were observed in the airglow over the Northeastern Brazil
- Analyses including reverse ray tracing suggested the eclipse as the likely source for one observed medium-scale gravity wave

Supporting Information:
- Supporting Information S1

Correspondence to:
I. Paulino,
igo.paulino@df.ufcg.edu.br

Citation:
Paulino, I., Figueiredo, C. A. O. B., Rodrigues, F. S., Buriti, R. A., Wrasse, C. M., Paulino, A. R., et al. (2020). Atmospheric gravity waves observed in the nightglow following the 21 August 2017 total solar eclipse. *Geophysical Research Letters*, *47*, e2020GL088924. https://doi.org/10.1029/2020GL088924

Received 20 MAY 2020
Accepted 13 JUL 2020
Accepted article online 19 AUG 2020

Abstract

Nighttime airglow images observed at the low-latitude site of São João do Cariri (7.4°S, 36.5°W) showed the presence of a medium-scale atmospheric gravity wave (AGW) associated with the 21 August 2017 total solar eclipse. The AGW had a horizontal wavelength of ~1,618 km, observed period of ~152 min, and propagation direction of ~200° clockwise from the north. The spectral characteristics of this wave are in good agreement with theoretical predictions for waves generated by eclipses. Additionally, the wave was reverse ray-traced, and the results show its path crossing the Moon's shadow of the total solar eclipse in the tropical North Atlantic ocean at stratospheric altitudes. Investigation about potential driving sources for this wave indicates the total solar eclipse as the most likely candidate. The optical measurements were part of an observational campaign carried out to detect the impact of the August 21 eclipse in the atmosphere at low latitudes.

Plain Language Summary

The Moon's shadow during a total solar eclipse introduces horizontal temperature gradients in the atmosphere and screens the ozone layer from solar heating. The shadow also travels supersonically, producing instabilities that can generate the so-called atmospheric gravity wave (AGW). AGWs associated with eclipses are expected to have periodic oscillations with periods ranging from just a few minutes to hours. Additionally, these AGWs can have horizontal wavelengths as large as thousands of kilometers. It is also possible to estimate the propagation path of the AGWs into the atmosphere by solving a system of equations that govern their propagation. This methodology is similar to that of tracing a ray of light that propagates in a varying environment. In the present work, an AGW in the northeast of Brazil was observed with spectral characteristics that indicate association with the 21 August 2017 total solar eclipse. In addition, the ray path matched the Moon's shadow in the stratosphere corroborating with the observational inferences. The AGW was observed by optical instruments during the nighttime, more than 3 h after the end of the eclipse and over 2,000 km away from the Moon's shadow.

1. Introduction

Wind shear, convection, and topography are often cited as the main sources of atmospheric gravity waves (AGWs) (e.g., Clemesha & Batista, 2008; Vadas et al., 2009, and references therein). However, events capable of creating disturbances in vertical pressure gradient and gravity balance might also induce the generation of AGWs. A solar eclipse produces a strong horizontal gradient of temperature and ionization flux in the atmosphere across the sunlit and covered areas. Additionally, the umbra moves supersonically, creating instabilities at different levels of the atmosphere which generates a wide spectum of AGWs (e.g., Fritts & Luo, 1993, and references therein). More details on the generation of gravity waves and acoustic gravity waves during an eclipse can be found in Knížová and Mošna (2011), who used plain language to explain this process.

After a series of publications about the generation of gravity waves by solar eclipses in the beginning of the 1970s decade (Chimonas & Hines, 1970; 1971; Chimonas, 1974), several experiments were carried out to

©2020. American Geophysical Union. All Rights Reserved.

investigate the characteristics of these gravity waves in the neutral atmosphere and their manifestation as traveling ionospheric disturbances (TIDs) in the ionosphere. The early experiments included observation of the solar eclipse on 7 March 1970 over the central and east coast of North America, which showed only some agreement between observations and theoretical predictions (e.g., Arendt, 1972; Davis & Da Rosa, 1970; Lerfald et al., 1972; Sears, 1972).

Several other experiments followed up trying to reconcile observations and theories related to AGWs and TIDs induced by eclipses (e.g., Beer & May, 1972; Frost & Clark, 1973). For instance, the experiments performed on 30 June 1973 identified AGWs and TIDs that were likely associated with the total solar eclipse that was observed crossing central Africa (e.g., Anderson & Keefer, 1975; Broche & Crochet, 1975; Jones & Bogart, 1975; Schödel et al., 1973). On 23 October 1976, AGWs and TIDs were also observed in South Australia associated with the eclipse (e.g., Beer et al., 1976). A few years later, on 26 February 1979, an eclipse was observed over North America and Greenland, and new studies on the ionospheric responses to eclipses were conducted (e.g., Narcisi et al., 1983).

During the 1980s, only two solar total eclipses crossed the continental areas: one on 16 February 1980 over Africa and Asia and another on 29 March 1987 over Africa. Again, AGWs and TIDs were observed during those events (e.g., Hanuise et al., 1982; Mohanakumar & Sankaranarayanan, 1982). In the 1990s, five eclipses were observed over inhabited areas (11 July 1991, 03 November 1994, 24 October 1995, 8 and 9 March 1997, and 11 August 1999). Unfortunately, only a few AGW/TID experiments were performed during those events (e.g., Altadill et al., 2001; Aplin & Harrison, 2003; Jones et al., 2004). In the past two decades at least 10 total solar eclipses occurred (21 June 2001, 04 December 2002, 08 April 2005, 29 March 2006, 01 August 2008, 21 and 22 July 2009, 13 and 14 November 2012, 03 November 2013, 21 August 2017, and 02 July 2019) over continental areas which allowed important ground-based observation of AGWs and TIDs (e.g., Afraimovich et al., 2007; Amabayo et al., 2014; Chen et al., 2011; Paul et al., 2011; Kumar et al., 2016a; Kumar et al., 2016b; Paulino et al., 2018; Vargas, 2019; Zerefos et al., 2007).

From the observations, several aspects of AGWs and TIDs induced by eclipses were learned. For instance, it was found that bow waves, generated by the Moon's shadow traveling at a supersonic speed, could be detected in parameters of neutral atmosphere and ionosphere. It was also found that periodic AGWs/TIDs with periods ranging from a few up to tens of minutes and wavelength extending up to a thousand kilometers could be observed during eclipse events. It must be pointed out that the spectral characteristics of the observed AGWs/TIDs depend on the distance where they were measured to the umbra of the eclipse. Furthermore, the wind system and the dissipative processes impose a natural filtering system, which limits the observable spectrum of AGWs at different atmospheric levels.

The total solar eclipse on 21 August 2017 presented a major opportunity to advance the understanding of the characteristics of AGWs (e.g., Coster et al., 2017, and references therein) and other atmospheric phenomena associated with the eclipse. The path of the umbra crossed the continental United States (e.g., McInerney et al., 2018) and allowed, perhaps, the most comprehensive set of experiments to be conducted to date.

In addition to the experiments in the United States, a multi-instrumented campaign of observations was carried out in the Northeast region of Brazil. The experiment was performed to determine the effects of the 21 August 2017 eclipse in the upper atmosphere at low latitudes including the occurrences of AGWs. Of particular importance is that the geographical location of the instruments operated during the campaign that allowed, for the first time, this type of nighttime observations. Signatures of gravity waves induced by eclipses have, however, already been observed in the rotational temperature during the night of 29 March 2006 (Aushev et al., 2008).

In the present work, the main results of the observations made by an all-sky imager located at São João do Cariri (7.4°S, 36.5°W, dip angle: 11°S) are presented and discussed. The imager detected a medium-scale AGW just 3 h after the end of eclipse, which occurred over the Atlantic ocean around 21:04 universal time (UT). The observed wave shows spectral characteristics and propagation direction that are compatible with their generation by an eclipses. Additionally, the potential propagation path of the AGW was derived using reverse ray tracing, and it was found that the position of the likely source is within the region of the umbra in the stratosphere. Finally, observations of horizontal winds made at the same site using a Fabry-Perot Interferometer also indicate signatures of large-scale gravity waves in the thermosphere associated with the eclipse (Harding et al., 2018), which reinforces that AGWs induced by the 21 August 2017 solar eclipse can be observed far away from its source.

2. Image Analysis and Results

Coordinated multi-instrumented observations of the upper atmosphere were made around the total solar eclipse of 21 August 2017 in the Northeast region of Brazil. The main objective of those observations was the detection of gravity waves and ionospheric disturbance associated with the eclipse. The network of instruments included: (a) three digisondes (e.g., Batista et al., 2017) located at São Luís (2.58°S, 44.2°W), Fortaleza (3.87°S, 38.41°W), and Cachoeira Paulista (22.67°S, 45.00°W); (b) one very high-frequency coherent backscatter radar (e.g., Rodrigues et al., 2013) at São Luís; (c) one meteor radar at Cachoeira Paulista (e.g., Paulino et al., 2012); (d) a network of fluxgate magnetometers distributed over the Brazilian territory (e.g., Denardini et al., 2018); (e) one Fabry-Perot interferometer at São João do Cariri (e.g., Makela et al., 2009); and (f) one all-sky airglow imager at São João do Cariri (e.g., Paulino et al., 2016). In this note, the investigation focused on the observations made by the all-sky imager. The main results of these observations were presented and discussed during the 42nd COSPAR Scientific Assembly (Paulino et al., 2018).

Images of the near-infrared OH and atomic Oxygen at 630.0 nm (OI6300) airglow emissions were collected during the night of 21 August 2017 every 2 min in order to properly monitor the AGW activity in the mesosphere and lower thermosphere (MLT) region after the end of the eclipse over the northeast of Brazil. The nominal height of the peak for the OH is ~87 km and the emission is proportional to the concentration of ozone and hydrogen. Therefore, it reflects the variation in the minor neutral constituents of the MLT. The nominal height of the OI6300 emission is ~250 km and the emission intensity is proportional to the concentration of O_2, N_2 and electrons in the thermosphere, which reflects variation in the concentration of ionospheric plasma. Our study focuses on OH images, where signatures of AGWs propagating southward and southwestward were identified after 00:00 UT.

To estimate horizontal AGW parameters (e.g., observed period, wavelength, and direction of propagation) in the OH images, two techniques were used: (1) the two-dimensional fast Fourier transform and cross-correlation spectrum (Garcia et al., 1997) and (2) analysis of keograms (e.g., Shiokawa et al., 2009). The first technique is often used to estimate parameters of small-scale gravity waves, and the second one is better used to study medium-scale gravity waves (e.g., Campos et al., 2016; Essien et al., 2018; Paulino et al., 2011).

The observations were complemented by additional numerical analysis. Reverse ray-tracing analysis was carried out to estimate the propagation path and to identify potential sources for the observed waves. The ray-tracing methodology is described in Vadas and Fritts (2009) and has already been used to investigate sources of AGWs in the equatorial region (e.g., Sivakandan et al., 2016, 2019). In summary, the ray path for AGWs propagating into the atmosphere is obtained solving the following set of equations:

$$\frac{dx_i}{dt} = V_i + \frac{\partial \omega_{Ir}}{\partial k_i} = V_i + c_{g_i} \tag{1}$$

and

$$\frac{dk_i}{dt} = -k_j \frac{\partial V_j}{\partial x_i} - \frac{\partial \omega_{Ir}}{\partial x_i}, \tag{2}$$

where x_i and k_i are the position and wavenumber of the wave at a given time, V_i is the neutral wind velocity, ω_{Ir} is the intrinsic frequency, and c_{g_i} is the group velocity. Repeated indices indicate summation, for example, "j." Temperature from the Naval Research Laboratory Mass Spectrometer Incoherent Scatter Radar 2000 (NRLMSIS-00, Picone et al., 2002) and winds from the Horizontal Wind Model 2014 (HWM-14, Drob et al., 2015) were used as input for the ray-tracing technique to calculate the reverse path of the gravity wave from surface up to the OH layer at 87 km altitude.

Analysis of the OH all-sky images show the occurrence of small- and medium-scale AGWs. The reverse ray-tracing results for small-scale AGWs (observed periods of ~10 min and horizontal wavelengths of ~30 km) showed that these waves reached tropospheric altitudes in the region near the observatory, that is, only a few hundreds of kilometers away. In addition to small-scale waves, two medium-scale gravity waves were identified, the first medium-scale AGW had a period of ~47 min, a horizontal wavelength of ~580 km, and propagated to the southeast. The result from the ray tracing indicated that the likely source was located

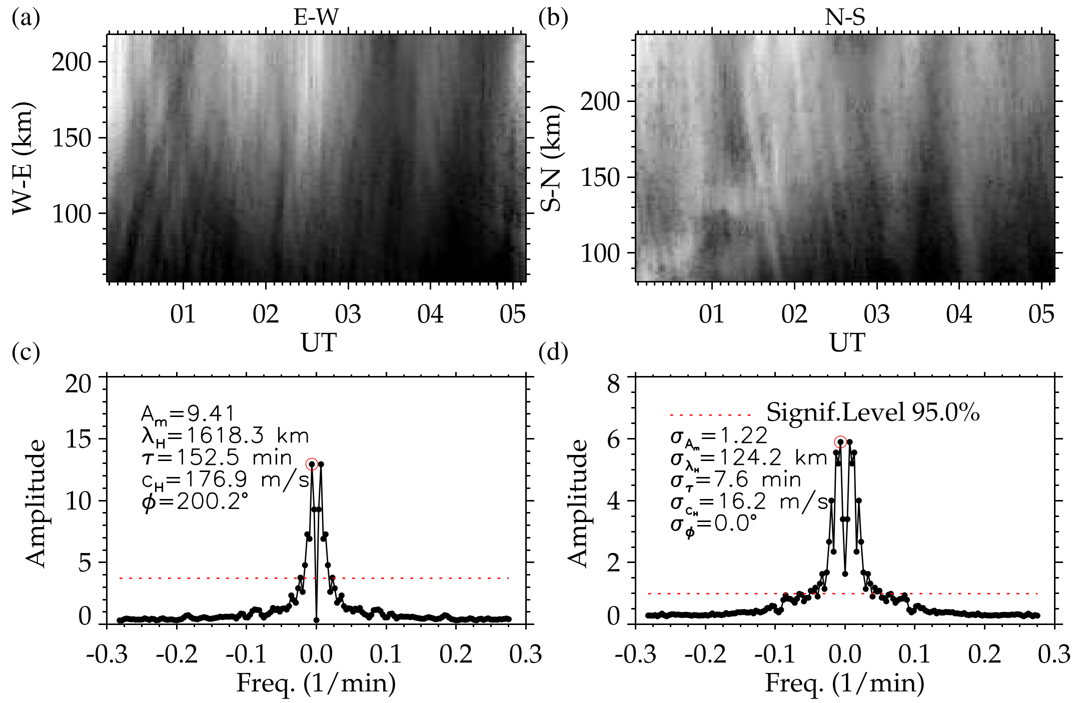

Figure 1. Keogram analysis for East–West (left side) and North–South (right side) on 21 and 22 August 2017. Panels (a) and (b) show the keograms from the airglow images. Panels (c) and (d) show the amplitude of the main oscillations.

over the ocean, to the northwest of the observatory. The second medium-scale AGW is going to be the focus of the present investigation as it was found to be related to the eclipse. It had a period of ~150 min, a horizontal wavelength of ~1,600 km and propagated southwestward (azimuth of 200° from the North clockwise). Therefore, the propagation direction suggested a connection with the eclipse.

Figure 1 shows the keogram results for the all-sky images when a medium-scale AGW was observed. Figure 1a,b shows the East–West (E-W) and North–South (N-S) cuts of the images as a function of the time (keograms), respectively. From the keograms, amplitudes (A_m), horizontal wavelength (λ_H), observed period (τ), horizontal phase speed (c_H), and propagation direction (ϕ) are derived. These parameters are indicated in Panel (c), which also shows the spectrum of fluctuations in the E-W direction. Panel (d) shows the spectrum of fluctuations in the N-S direction and the uncertainty in the derived parameter values. Details about the derivation of these parameters of AGWs from keograms can be found in appendix A of Figueiredo et al. (2018). One can see in Figure 1a one crest on the central portion of the keogram, whereas Figure 1b shows one crest in the beginning and one valley to wards the end part of the keogram. Note that, besides the medium-scale structure, the keograms also show other small oscillations.

Figure 2 shows the path of the medium-scale AGW derived from the reverse ray tracing assuming two distinct background wind patterns. The dashed red line represents the ray-tracing results for zero wind model. The solid green line represents the results for the HWM-14 winds. Comparison using zero wind and modeled wind gives an idea about the effect of the wind in changing the trajectory of the wave into the atmosphere. In the present case, only small differences were noted. Furthermore, the black heavy line shows the path of the Moon's shadow and the blue spots represent regions with cold clouds, which can indicate local instability. Cloud temperature information was obtained from Geostationary Operational Environmental Satellites from the infrared images of the clouds. The occurrence of cold clouds has been used to identify convection and potential sources of small-scale AGWs (Dare-Idowu et al., 2020). Colder clouds are located at higher altitudes, which leads to a higher potential for intense vertical motion, generation of instabilities, and, consequently, gravity waves. The color bar on the top of Figure 2 shows the temperature scale in degrees Celsius. The blue spots in Figure 2 indicate the occurrence of convection near the end of the eclipse path, in the Amazon region and over the North tropical Atlantic ocean. Note that the ray-tracing results show that the

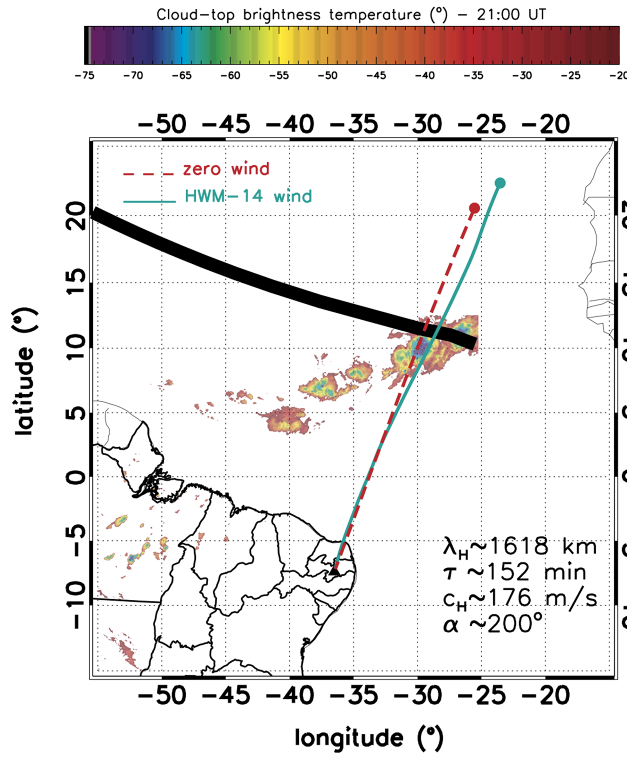

Figure 2. The ray path of the gravity wave on a geographical map. The red dashed line represents the ray path using zero wind condition and the solid green line represents the HWM-14 wind condition. The black heavy line represents the Moon's shadow. The rainbow spots represent clouds in which the estimated temperature is shown in the color bar on the top. Colder clouds are shown in violet and indicates deep convection and very high clouds. The black triangle indicates the position of the observatory at São João do Cariri.

path of the medium-scale AGW crossed the end of the eclipse and extended horizontally over 1,000 km to the northeast direction.

Figure 3 shows the results for the temporal evolution of the gravity wave ray path into the atmosphere. Again, results for the HWM-14 wind model and for zero winds converge to similar paths. The horizontal black line represents the altitude where the ray path crossed the Moon's shadow, which is around 34.4 km altitude, that is, in the stratospheric heights. These results show that this medium-scale gravity wave likely had its sources located over the north tropical Atlantic ocean.

3. Discussion

It was shown in Figure 1 that the medium-scale AGW started to be observed around 00:00 UT (21:00 local time) over São João do Cariri. This starting time is more than 3 h after the end of the eclipse over the Atlantic ocean. Using the horizontal phase speed of ~176 m/s derived from keograms, one can estimate that the wave traveled ~2,218 km in 3.5 h. The point in which the ray path of medium-scale AGW crossed the Moon's shadow (see Figure 2) is located at 10.98°N and 28.63°W and it is ~2,230 km away from the observatory. Therefore, the propagation speed suggests that the source of the observed AGW could be at this point. Besides the Moon's shadow, there is indication of convection around that region. Moreover, around the point in which the ray-path reached the troposphere, there is no indication of convection, which makes tropospheric source to be considered unlikely.

The next point to be analyzed is the vertical propagation of the medium-scale AGW derived from the reverse ray-tracing analysis. Figure 3 shows the vertical ray path of the medium-scale AGW inferred using HWM-14 winds and no winds for comparison purposes. The ray paths for the two cases are similar because the AGW had a high horizontal phase speed and it could easily escape from critical and turning levels in the atmosphere. Figure 3 shows that the wave would have traveled for more than five hours from the surface up to the OH layer and it would have crossed the Moon's shadow at around 34.4 km altitude and 21:06 UT (wind

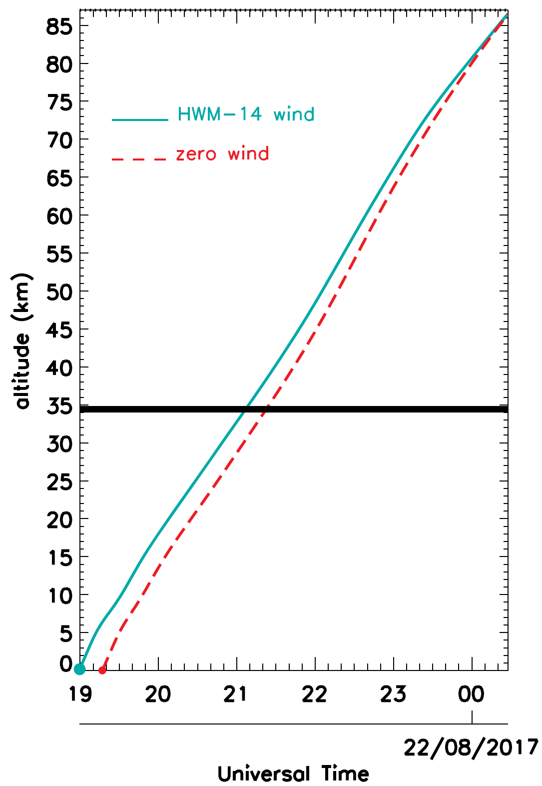

Figure 3. Extension of Figure 1 for the vertical propagation of the medium-scale atmospheric gravity wave against the time. The horizontal black line represents the altitude where the ray path of the waves crossed the Moon's shadow.

model condition). From this point onwards, it took more than 3 h for the wave to reach the OH layer altitude of ~87 km. Therefore, according to the ray-tracing results, potential source for the observed AGW would be located in the stratosphere (~34 km altitude) over 11°N and 28.5°W.

In general, deep convection clouds, like the ones that can be seen in Figure 2, near the end of the path of the eclipse extend up to a pressure level of about 70 hPa, which is approximately 17.7 km in altitude (e.g., Sherwood et al., 2004). So, one can wonder if such a structure could excite gravity waves in the stratosphere. Observations during the Spread-F experiment (SpreadFEx) campaign carried out also over Brazil in 2005 found similar convective plumes (Vadas et al., 2009). Vadas and Fritts (2009) calculated the effects of a single convective plume and small convective cluster that can be compared to the present case study. They found that the most dominant spectrum of AGWs generated by these plumes included small-scale gravity waves with a horizontal wavelength shorter than 400 km and reaching the OH layer altitudes within an hour. Therefore, the only possible way that the observed convective system could excite gravity waves in the stratosphere would be through body forcing producing secondary gravity waves in the stratosphere, which is unlikely according to the simulations made by Vadas and Fritts (2009).

Given the lack of plausible convection sources, the eclipse becomes a strong candidate as the source of AGWs along the path of the Moon's shadow by the screening of the ozone layer from solar heating. Predictions of AGWs generated by eclipse showed dominant periodicities in the atmospheric fields from 2 to 4 h (Fritts & Luo, 1993). This is in good agreement with the present observations. They have, however, calculated the horizontal scale of the structures more likely to be observed in the lower thermosphere to be over 5,000 km.

However, optical (FPI) observations by Aushev et al. (2008) also revealed periodicities associated with the 29 March 2006 total solar eclipse in good agreement with the present results. Additionally, a wide spectrum of TIDs has been observed during eclipses with periods ranging from a few minutes (e.g., Davis & Da Rosa, 1970) up to a couple of hours (e.g., Liu et al., 1998), which is close to the period of the observed medium-scale AGW.

Regarding the 21 August 2017 total solar eclipse more specifically, a temperature reduction of 1 K and increase by a factor of 2 in the ozone were predicted by the Whole Atmosphere Community Climate Model-eXtended (McInerney et al., 2018). As a result of these changes in the atmospheric composition and dynamics, large-scale disturbances (TIDs) were observed in the ionosphere associated with the eclipse (e.g., Coster et al., 2017). Finally, a wave-like signature of the bow wave generated by the eclipse was observed in the neutral winds by a Fabry-Perot interferometer over São João do Cariri (Harding et al., 2018) and over Carbondale (37.7 ^{o}N, 89.2 ^{o}W) using airglow red and green lines (Aryal et al., 2019).

4. Conclusions

In summary, a medium-scale AGW was detected associated with the 21 August 2017 eclipse using a unique experimental setup over the Brazilian territory. Of particular importance is that the wave was observed at low latitudes and about 2,000 km away from the eclipse path (umbra). The AGW was observed using an all-sky imager located in São João do Cariri approximately 3 h after the end of the eclipse. The wave had an observed period of ~2.5 h and a horizontal wavelength of ~1,620 km. Additionally, the observations showed that the wave propagated to the southwest with an azimuth of ~200° clockwise from the North.

The spectral characteristics of the observed wave match the theoretical prediction for AGW generated by solar eclipses. Furthermore, reverse ray-tracing simulations were performed and the results corroborate with potential wave sources located around 11°N, 28.5°W, and 34 km altitude, which was the position where the gravity wave ray path crossed the Moon's shadow in the stratosphere. This is the first time that a gravity wave generated by an eclipse was captured by an all-sky airglow camera in the MLT region during the nighttime. Finally, given the limitation in the number of eclipses observed with adequate instrumentation, the present work contributes to a better understanding of the effects of eclipses in atmospheric dynamics.

Authors Contribution

Authors' Contribution IP wrote the manuscript and did most of the airglow analysis. CAOBF performed the spectral analysis of the gravity waves and revised the manuscript. FSR revised the manuscript and interpretation. RAB contributed to running the experiments in São João do Cariri during the eclipse and revised the manuscript. CMW helped with the analysis and interpretation and revised the manuscript. ARP helped with the interpretation of the results and revised the manuscript. DB provided the database for the ray-tracing. HT, ISB, AFM, PPB, MAA, ERP, CMD, LML, RYCC and JJM supported the coordinated multi-instrumented observations during the eclipse and revised the manuscript.

Conflicts of Interest

The authors declare that they have no conflict of interest.

Acknowledgments
Airglow images from São João do Cariri can be accessed online in the portal of the "Estudo e Monitoramento Brasileiro do Clima Espacial" (EMBRACE/INPE) at a website (www.inpe.br/spaceweather/). The cloud top brightness temperature maps were provided by the Center for Weather Forecasting and Climate Studies (CPTEC/INPE) at a website (https://satelite.cptec.inpe.br/acervo). Ray-tracing calculations have been uploaded at a website (https://doi.org/10.6084/m9.figshare.12707900). I. Paulino, C. M. Wrasse, A. R. Paulino, E. R. de Paula, C. M. Denardini, I. S. Batista, and D. Barros thank the Conselho Nacional de Desenvolvimento Científico e Tecnológico (CNPq) for the support under contracts 303511/2017-6, 307653/2017-0, 460624/2014-8, 202531/2019-0, 303643/2017-0, 306844/2019-2, and 300974/2020-5. I. Paulino, A. F. Medeiros, A. R. Paulino, R. A. Buriti, P. Batista, and C. M. Denardini thank the Fundação de Amparo à Pesquisa do Estado da Paraíba by the PRONEX grant (Termo de Concessão e Aceitação Financeira 002/2019). A. R. Paulino thanks the Coordenação de Aperfeiçoamento de Pessoal de Nível Superior (CAPES) for the scholarship. F. S. Rodrigues would like to thank for the support from NSF (Award AGS-1915925). C. A. O. B. Figueiredo thanks the Fundação de Amparo à Pesquisa do Estado de São Paulo (FAPESP) for kindly providing financial support through the process number 2018/09066-8. Work at Illinois was supported by NSF grant AGS 16-51298.

References

Afraimovich, E. L., Voeykov, S. V., Perevalova, N. P., Vodyannikov, V. V., Gordienko, G. I., Litvinov, Y. G., & Yakovets, A. F. (2007). Ionospheric effects of the March 29, 2006, solar eclipse over Kazakhstan. *Geomagnetism and Aeronomy*, *47*(4), 461–469. https://doi.org/10.1134/S0016793207040068

Altadill, D., Solé, J. G., & Apostolov, E. M. (2001). Vertical structure of a gravity wave like oscillation in the ionosphere generated by the solar eclipse of August 11, 1999. *Journal of Geophysical Research*, *106*(A10), 21,419–21,428. https://doi.org/10.1029/2001JA900069

Amabayo, E., Anguma, S., & Jurua, E. (2014). Tracking the ionospheric response to the solar eclipse of November 03, 2013. *International Journal of Atmospheric Sciences*, *2014*, 1–10. https://doi.org/10.1155/2014/127859

Anderson, R. C., & Keefer, D. R. (1975). Observation of the temperature and pressure changes during the 30 June 1973 solar eclipse. *Journal of the Atmospheric Sciences*, *1*, 228–231. https://doi.org/10.1175/1520-0469(1975)032<0228:OOTTAP>2.0.CO;2

Aplin, K., & Harrison, R. (2003). Meteorological effects of the eclipse of 11 August 1999 in cloudy and clear conditions. *Proceedings of the Royal Society of London. Series A: Mathematical, Physical and Engineering Sciences*, *459*(2030), 353–371. https://doi.org/10.1098/rspa.2002.1042

Arendt, P. (1972). Ionospheric undulations during the solar eclipse of 7 March 1970. *Journal of Atmospheric and Terrestrial Physics*, *34*(4), 719–725. https://doi.org/10.1016/0021-9169(72)90159-6

Aryal, S., Geddes, G., Finn, S. C., Mrak, S., Galkin, I., Cnossen, I., et al. (2019). Multispectral and multi-instrument observation of TIDs following the total solar eclipse of 21 August 2017. *Journal of Geophysical Research: Space Physics*, *124*, 3761–3774. https://doi.org/10.1029/2018JA026333

Aushev, V. M., Lyahov, V. V., López-González, M. J., Shepherd, M. G., & Dryn, E. A. (2008). Solar eclipse of the 29 March 2006: Results of the optical measurements by MORTI over Almaty (43.03 °n, 76.58 °e). *Journal of Atmospheric and Solar-Terrestrial Physics*, *70*(7), 1088–1101. https://doi.org/10.1016/j.jastp.2008.01.018

Batista, I. S., Candido, C. M. N., Souza, J. R., Abdu, M. A., de Araujo, R. C., Resende, L. C. A., & Santos, A. M. (2017). F3 layer development during quiet and disturbed periods as observed at conjugate locations in Brazil: The role of the meridional wind. *Journal of Geophysical Research: Space Physics*, *122*, 2361–2373. https://doi.org/10.1002/2016JA023724

Beer, T., Goodwin, G. L., & Hobson, G. J. (1976). Atmospheric gravity wave production for the solar eclipse of October 23, 1976. *Nature*, *264*(5585), 420–421. https://doi.org/10.1038/264420a0

Beer, T., & May, A. N. (1972). Atmospheric gravity waves to be expected from the solar eclipse of June 30, 1973. *Nature*, *240*(5375), 30–32. https://doi.org/10.1038/240030a0

Broche, P., & Crochet, M. (1975). Generation of atmospheric gravity waves by the 30 June 1973 solar eclipse in Africa. *Journal of Atmospheric and Terrestrial Physics*, *37*(10), 1371–1374. https://doi.org/10.1016/0021-9169(75)90130-0

Campos, J., Paulino, I., Wrasse, C., Medeiros, A. F., Paulino, A. R., & Buriti, R. A. (2016). Observations of small-scale gravity waves in the equatorial upper mesosphere. *Brazilian Journal of Geophysics*, *34*(4), 469–477. https://doi.org/10.22564/rbgf.v34i4.876

Chen, G., Zhao, Z., Zhang, Y., Yang, G., Zhou, C., Huang, S., et al. (2011). Gravity waves and spread Es observed during the solar eclipse of 22 July 2009. *Journal of Geophysical Research*, *116*, A09314. https://doi.org/10.1029/2011JA016720

Chimonas, G. (1974). Internal gravity-wave motions induced in the Earth's atmosphere by a solar eclipse. In *The upper atmosphere in motion* (pp. 708–714). Washington, DC: American Geophysical Union (AGU). https://doi.org/10.1029/GM018p0708

Chimonas, G., & Hines, C. O. (1970). Atmospheric gravity waves induced by a solar eclipse. *Journal of Geophysical Research*, *75*(4), 875–875. https://doi.org/10.1029/JA075i004p00875

Chimonas, G., & Hines, C. O. (1971). Atmospheric gravity waves induced by a solar eclipse, 2. *Journal of Geophysical Research*, *76*(28), 7003–7005. https://doi.org/10.1029/JA076i028p07003

Clemesha, B., & Batista, P. (2008). Gravity waves and wind-shear in the {MLT} at 23°S. *Advances in Space Research*, *41*(9), 1472–1477. https://doi.org/10.1016/j.asr.2007.03.085

Coster, A. J., Goncharenko, L., Zhang, S.-R., Erickson, P. J., Rideout, W., & Vierinen, J. (2017). GNSS observations of ionospheric variations during the 21 August 2017 solar eclipse. *Geophysical Research Letters*, *44*, 12,041–12,048. https://doi.org/10.1002/2017GL075774

Dare-Idowu, O., Paulino, I., Figueiredo, C. A. O. B., Medeiros, A. F., Buriti, R. A., Paulino, A. R., & Wrasse, C. M. (2020). Investigation of sources of gravity waves observed in the Brazilian equatorial region on 8 April 2005. *Annales Geophysicae*, *38*(2), 507–516. https://doi.org/10.5194/angeo-38-507-2020

Davis, M. J., & Da Rosa, A. V. (1970). Possible detection of atmospheric gravity waves generated by the solar eclipse. *Nature*, *226*(5251), 1123–1123. https://doi.org/10.1038/2261123a0

Denardini, C. M., Chen, S. S., Resende, L. C. A., Moro, J., Bilibio, A. V., Fagundes, P. R., et al. (2018). The embrace magnetometer network for South America: Network description and its qualification. *Radio Science*, *53*, 288–302. https://doi.org/10.1002/2017RS006477

Drob, D. P., Emmert, J. T., Meriwether, J. W., Makela, J. J., Doornbos, E., Conde, M., et al. (2015). An update to the Horizontal Wind Model (HWM): The quiet time thermosphere. *Earth and Space Science*, *2*, 301–319. https://doi.org/10.1002/2014EA000089

Essien, P., Paulino, I., Wrasse, C. M., Campos, J. A. V., Paulino, A. R., Medeiros, A. F., et al. (2018). Seasonal characteristics of small- and medium-scale gravity waves in the mesosphere and lower thermosphere over the brazilian equatorial region. *Annales Geophysicae*, *36*(3), 899–914. https://doi.org/10.5194/angeo-36-899-2018

Figueiredo, C. A. O. B., Takahashi, H., Wrasse, C. M., Otsuka, Y., Shiokawa, K., & Barros, D. (2018). Medium-scale traveling ionospheric disturbances observed by detrended total electron content maps over Brazil. *Journal of Geophysical Research: Space Physics*, *123*, 2215–2227. https://doi.org/10.1002/2017JA025021

Fritts, D. C., & Luo, Z. (1993). Gravity wave forcing in the middle atmosphere due to reduced ozone heating during a solar eclipse. *Journal of Geophysical Research*, *D2*, 3011–3021. https://doi.org/10.1029/92JD02391

Frost, A. D., & Clark, R. R. (1973). Predicted acoustic gravity wave enhancement during the solar eclipse of June 30, 1973. *Journal of Geophysical Research*, *78*(19), 3995–3997. https://doi.org/10.1029/JA078i019p03995

Garcia, F. J., Taylor, M. J., & Kelley, M. C. (1997). Two-dimensional spectral analysis of mesospheric airglow image data. *Applied Optics*, *36*(29), 7374–7385. https://doi.org/10.1364/AO.36.007374

Hanuise, C., Broche, P., & Ogubazghi, G. (1982). HF Doppler observations of gravity waves during the 16 February 1980 solar eclipse. *Journal of Atmospheric and Terrestrial Physics*, *44*(11), 963–966. https://doi.org/10.1016/0021-9169(82)90060-5

Harding, B. J., Drob, D. P., Buriti, R. A., & Makela, J. J. (2018). Nightside detection of a large-scale thermospheric wave generated by a solar eclipse. *Geophysical Research Letters*, *45*, 3366–3373. https://doi.org/10.1002/2018GL077015

Jones, B. W., & Bogart, R. S. (1975). Eclipse induced atmospheric gravity waves. *Journal of Atmospheric and Terrestrial Physics*, *37*(9), 1223–1226. https://doi.org/10.1016/0021-9169(75)90194-4

Jones, T. B., Wright, D. M., Milner, J., Yeoman, T. K., Reid, T., Chapman, P. J., & Senior, A. (2004). The detection of atmospheric waves produced by the total solar eclipse of 11 August 1999. *Journal of Atmospheric and Solar-Terrestrial Physics*, *66*(5), 363–374. https://doi.org/10.1016/j.jastp.2004.01.029

Knížová, P. K., & Mošna, Z. (2011). Acoustic-gravity waves in the ionosphere during solar eclipse events. In M. G. Beghi (Ed.), *Acoustic waves - from microdevices to helioseismology* (pp. 14). IntechOpen. https://doi.org/10.5772/19722

Kumar, K. V., Maurya, A. K., Kumar, S., & Singh, R. (2016a). 22 July 2009 total solar eclipse induced gravity waves in ionosphere as inferred from GPS observations over EIA. *Advances in Space Research*, *58*(9), 1755–1762. https://doi.org/10.1016/j.asr.2016.07.019

Kumar, S., Kumar, A., Maurya, A. K., & Singh, R. (2016b). Changes in the D region associated with three recent solar eclipses in the South Pacific region. *Journal of Geophysical Research: Space Physics*, *121*, 5930–5943. https://doi.org/10.1002/2016JA022695

Lerfald, G., Jurgens, R., Vesecky, J., & Washburn, T. (1972). Traveling ionospheric disturbances observed near the time of the solar eclipse of 7 March 1970. *Journal of Atmospheric and Terrestrial Physics*, *34*(4), 733–741. https://doi.org/10.1016/0021-9169(72)90161-4

Liu, J. Y., Hsiao, C. C., Tsai, L. C., Liu, C. H., Kuo, F. S., Lue, H. Y., & Huang, C. M. (1998). Vertical phase and group velocities of internalgravity waves derived from ionograms during the solareclipse of 24 October 1995. *Journal of Atmospheric and Solar-Terrestrial Physics*, *60*(17), 1679–1686. https://doi.org/10.1016/S1364-6826(98)00103-5

Makela, J. J., Meriwether, J. W., Lima, J. P., Miller, E. S., & Armstrong, S. J. (2009). The remote equatorial nighttime observatory of ionospheric regions project and the international heliospherical year. *Earth, Moon, and Planets*, *104*(1), 211–226. https://doi.org/10.1007/s11038-008-9289-0

McInerney, J. M., Marsh, D. R., Liu, H.-L., Solomon, S. C., Conley, A. J., & Drob, D. P. (2018). Simulation of the 21 August 2017 solar eclipse using the whole atmosphere community climate model-extended. *Geophysical Research Letters*, *45*, 3793–3800. https://doi.org/10.1029/2018GL077723

Mohanakumar, K., & Sankaranarayanan, D. (1982). Solar eclipse of February 16, 1980 - it's effect on meteorological parameters. *Proceedings of the Indian National Science Academy*, *48A*, 209.

Narcisi, R., Bailey, A., Federico, G., & Wlodyka, L. (1983). Positive and negative ion composition measurements in the D- and E-regions during the 26 February 1979 solar eclipse. *Journal of Atmospheric and Terrestrial Physics*, *45*(7), 461–478. https://doi.org/10.1016/S0021-9169(83)81107-6

Paul, A., Das, T., Ray, S., Das, A., Bhowmick, D., & DasGupta, A. (2011). Response of the equatorial ionosphere to the total solar eclipse of 22 July 2009 and annular eclipse of 15 January 2010 as observed from a network of stations situated in the Indian longitude sector. *Annales Geophysicae*, *29*(10), 1955–1965. https://doi.org/10.5194/angeo-29-1955-2011

Paulino, A. R., Batista, P. P., & Clemesha, R. (2012). Lunar tides in the mesosphere and lower thermosphere over Cachoeira Paulista (22.7°S); 45.0°W). *Journal of Atmospheric and Solar-Terrestrial Physics*, *78-79*, 31–36. https://doi.org/10.1016/j.jastp.2011.04.018

Paulino, I., Lima, L., Marcos Denardini, C., Buriti, R., Paulino, A. R., Batista, P., et al. (2018). Observations of gravity waves in the airglow during the night of 21 August 2017 solar total eclipse over Brazil, *42nd COSPAR Scientific Assembly* (vol. 42, pp. C1.1–30-18).

Paulino, I., Medeiros, A. F., Vadas, S. L., Wrasse, C. M., Takahashi, H., Buriti, R. A., et al. (2016). Periodic waves in the lower thermosphere observed by OI630 nm airglow images. *Annales Geophysicae*, *34*(2), 293–301. https://doi.org/10.5194/angeo-34-293-2016

Paulino, I., Takahashi, H., Medeiros, A. F., Wrasse, C. M., Buriti, R. A., Sobral, J. H. A., & Gobbi, D. (2011). Mesospheric gravity waves and ionospheric plasma bubbles observed during the COPEX campaign. *Journal of Atmospheric and Solar-Terrestrial Physics*, *11*, 1575–1580. https://doi.org/10.1016/j.jastp.2010.12.004

Picone, J. M., Hedin, A. E., Drob, D. P., & Aikin, A. C. (2002). NRLMSISE-00 empirical model of the atmosphere: Statistical comparisons and scientific issues. *Journal of Geophysical Research*, *107*(A12), 1468. https://doi.org/10.1029/2002JA009430

Rodrigues, F. S., Shume, E. B., de Paula, E. R., & Milla, M. (2013). Equatorial 150 km echoes and daytime F region vertical plasma drifts in the Brazilian longitude sector. *Annales Geophysicae*, *31*(10), 1867–1876. https://doi.org/10.5194/angeo-31-1867-2013

Schödel, J. P., Klostermeyer, J., & Röttger, J. (1973). Atmospheric gravity wave observations after the solar eclipse of June 30, 1973. *Nature*, *245*(5420), 87–88. https://doi.org/10.1038/245087a0

Sears, R. (1972). Ionospheric HF Doppler dispersion during the eclipse of 7 March 1970 and TID analysis. *Journal of Atmospheric and Terrestrial Physics*, *34*(4), 727–732. https://doi.org/10.1016/0021-9169(72)90160-2

Sherwood, S. C., Minnis, P., & McGill, M. (2004). Deep convective cloud-top heights and their thermodynamic control during CRYSTAL-FACE. *Journal of Geophysical Research*, *109*, D20119. https://doi.org/10.1029/2004JD004811

Shiokawa, K., Otsuka, Y., & Ogawa, T. (2009). Propagation characteristics of nighttime mesospheric and thermospheric waves observed by optical mesosphere thermosphere imagers at middle and low latitudes. *Earth, Planets and Space*, *61*, 479–491. https://doi.org/10.1186/BF03353165

Sivakandan, M., Paulino, I., Ramkumar, T. K., Taori, A., Patra, A. K., Sripathi, S., et al. (2019). Multi-instrument investigation of troposphere-ionosphere coupling and the role of gravity waves in the formation of equatorial plasma bubble. *Journal of Atmospheric and Solar-Terrestrial Physics*, *189*, 65–79. https://doi.org/10.1016/j.jastp.2019.04.006

Sivakandan, M., Paulino, I., Taori, A., & Niranjan, K. (2016). Mesospheric gravity wave characteristics and identification of their sources around spring equinox over Indian low latitudes. *Atmospheric Measurement Techniques*, *9*(1), 93–102. https://doi.org/10.5194/amt-9-93-2016

Vadas, S. L., & Fritts, D. C. (2009). Reconstruction of the gravity wave field from convective plumes via ray tracing. *Annales Geophysicae*, *27*(1), 147–177. https://doi.org/10.5194/angeo-27-147-2009

Vadas, S. L., Taylor, M. J., Pautet, P.-D., Stamus, P. A., Fritts, D. C., Liu, H.-L., et al. (2009). Convection: The likely source of the medium-scale gravity waves observed in the OH airglow layer near Brasilia, Brazil, during the SpreadFEx campaign. *Annales Geophysicae*, *27*(1), 231–259. https://doi.org/10.5194/angeo-27-231-2009

Vargas, F. (2019). Gravity Wave Activity over the Andes Lidar Observatory (ALO) Generated by the July 2, 2019 Full Solar Eclipse Observed in Chile. *Earth and Space Science Open Archive*, 1. https://doi.org/10.1002/essoar.10501368.1

Zerefos, C. S., Gerasopoulos, E., Tsagouri, I., Psiloglou, B. E., Belehaki, A., Herekakis, T., et al. (2007). Evidence of gravity waves into the atmosphere during the March 2006 total solar eclipse. *Atmospheric Chemistry and Physics*, *7*(18), 4943–4951. https://doi.org/10.5194/acp-7-4943-2007